INFLUENCE OF IMPULS FORCES ON PARTICLE BEHAVIOUR IN GAS-PARTICLE MIXTURE FLOW IN HORIZONTAL TUBES

by

Goran ŽIVKOVIĆ

Original scientific paper
UDC: 533.6.011
BIBLID: 0350–9836, *2* (1998), 1, 33–55

In this paper the three-dimensional model of gas-particle mixture turbulent flow in horizontal tubes and channels, as well as in complex pipes with bends was developed, in order to make a tool for analyzing processes in pneumatic conveying systems. Gas turbulence was modeled using k-ε model of turbulence. In getting the numerical solution for the gas phase a finite volume discretization scheme was used. Iterative procedure was based on SIMPLE algorithm. Numerical code CAST for single phase flow with colocated grid represented the basis for it. The presence of dispersed phase and its influence on gas phase was modeled by adding one additional source term in the equations of the gas phase (PSI-CELL method). Dispersed phase was treated by the Lagrangian approach. For particle motion LSD model was used [13]. The concept of parcel, the computational particle which represents the ensemble of real particles with the same performances was adopted. Particles were treated as ideal spheres. Beside the drag and the gravitational forces, the lift forces due to the particle rotation and the gradient of the gas velocity field were included in calculation. Special attention was devoted to the models of particle collision with the rough wall and mutual collisions of particles. On this way the use of the model on flows in which the particle-gas mass ratio is high was enabled. The stochastical approach was adopted, by which all the parameters with the stochastic nature in reality retain it in the model also. The modeling of roughness was performed by changing the wall surface with the 'virtual plane', whose position is detemined with the angle of inclination around horizontal axes (modeling of roughness height), and the angle of rotation around vertical axes (modeling of orientation of roughnes in space). The first one was obeyed to the normal, and the second one to the uniform distribution. In the model of collisions between the particles the collision probability was calculated, and on this basis it was stochastically determined whether the collision of the particular particle with some other would happen or not. The calculation were made for particles of the mean diameter in the range 40–500 μm and for the particle-gas mass ratio 0–5. For the whole ensemble of particles in the flow field the log-normal distribution of their diameters was adopted. The results of calculation were compared with the experimental results available in literature. For the profiles of gas velocity and pressure drop excellent agreement was achieved. The agreement of the concentration profiles of the dispersed phase was good, except for the regions of high particle concentration near the wall.

Introduction

Pneumatic conveying is one of the oldest and cheapest way to transport powders over long but also short distances. Nevertheless, due to the great complexity of two-phase

flow in the different pipe elements, there was no in the past exact mathematical description of the processes in pneumatic conveying systems. Therefore, the lay-out of pneumatic conveying systems was based on data empirically obtained in laboratory or pilot-scale plants.

The particle motion is affected by:

- gas turbulence (dispersion, Lee and Durst [4]);
- transverse lift forces;
- gravitational settling in horizontal sections of pipelines;
- collision of the particles with the rough wall;
- particle-particle collisions;
- particle rotation;
- inertial behaviour in pipe bends.

This paper mainly deals with the analysis and modeling of impulse forces (particle-wall and particle-particle collisions) which act on particles during their motion through pipes. It is part of the ample task of getting more insight into the process using numerical simulation, in the course of developing the full model of pneumatic conveying in complex pipe systems.

Due to the large influence of gravitation on solid phase concentration profile in horizontal tubes even the simple flow configuration is three-dimensional in nature. The present paper reports on developments to establish a 3-D numerical code for simulations of pneumatic conveying in pipe systems where the wall roughness, particle-particle collisions and the influence of the solid phase on the gas flow is considered. Finally, the numerical code will allow numerical predictions of the flow structure in complete pipe systems and the resulting pressure drop.

Mathematical model of two-phase gas-particle flow

Since the main aim of the work was to model processes in the pneumatic conveying systems, which works in the steady-state regime, the stationary model was developed. The gas phase was treated by Eulerian approach, that is, the gas parameters were defined as functions of spatial coordinates. On the other side, dispersed phase was treated by Lagrangian approach, which means that parameters of every particle are functions of time [8]. Although that means that in the equations of particle motion time appears explicitly, as the outcome of enormous number of particles in the flow domain, the mean characteristics of dispersed phase in sufficiently long period do not change, so we can consider them as stationary (quasistationary).

As the result of the modeling one should get the fields of gas mean velocities, its turbulent energy and dissipation, pressure drop, as well as mean velocities, mass flux and concentration for dispersed phase.

For coupling of phases the PSI-in-CELL method, Crowe [5], was chosen. By this method the whole influence of dispersed phase on gas phase was performed through additional terms in equations which describe the gas phase. This could be done only by introducing two assumptions: 1) Total volume of particles is negligible in comparison

with the volume of the flow domain. This assumption is quite reasonable, since even in mixtures where particle to gas mass loading ratio is about one (which in pneumatic conveying can be considered as mixtures with large particle concentration) total volume of particle does not exceed 0.05%. On this way gas phase can still be treated as Newtonian fluid; 2) boundary conditions influence directly only gas phase (and dispersed phase through coupling of phases). On this way the model of gas flow in two phase mixture is reduced to single-phase model, in which the whole influence of the other phase is performed through the additional source terms.

Turbulence is modeled by standard k-ε model [1, 2, 3]. Therefore, the basic equations for gas flow (in tensor notation) are:

$$\frac{\partial(\rho U_i)}{\partial x_i} = 0 \qquad \text{(Continuity)} \qquad (1)$$

$$\frac{\partial}{\partial x_j}(\rho U_i U_j + \overline{\rho u_i u_j} - \mu \frac{\partial}{\partial x_j} U_i) = -\frac{\partial P}{\partial x_i} + S_i^P \qquad \text{(Navier-Stokes)} \qquad (2)$$

$$\frac{\partial}{\partial x_j}\left[\partial U_j k - \frac{\mu_{ef}}{\sigma_k}\frac{\partial k}{\partial x_j}\right] = P_k - \rho\varepsilon + S_k^P \qquad \text{(Turbulent kinetic energy)} \qquad (3)$$

$$\frac{\partial}{\partial x_j}\left[\rho U_j \varepsilon - \frac{\mu_{ef}}{\sigma_\varepsilon}\frac{\partial \varepsilon}{\partial x_j}\right] = \frac{\varepsilon}{k}(C_{\varepsilon 1} P_k - C_{\varepsilon 2}\rho\varepsilon) + S_\varepsilon^P \qquad \text{(Turbulent dissipation)} \qquad (4)$$

$$\mu_{ef} = \mu_t + \mu \qquad \mu_t = \frac{C_\mu \rho k^2}{\varepsilon} \qquad (5)$$

Source terms due to the presence of particles are denoted by index p, and are given by [4]:

$$S_i^P = \frac{1}{V t_{tot}} \sum_n m_{pn}(U_i^{out} - U_i^{in} - g_i \Delta t) \quad S_k^P = \overline{s_{u_i}^P u_i} \quad S_\varepsilon^P = C_3 \frac{\varepsilon}{k} S_k^P \qquad (6)$$

The sumation was performed over the all particles which pass through considered control volume in period t_{tot}. V represents a volume of the considered control volume. Standard coefficients of the k-ε model were used, and are given in the next table:

C_μ	$C_{\varepsilon 1}$	$C_{\varepsilon 2}$	C_3	σ_k	σ_ε
0.09	1.44	1.92	0.7	1.0	1.3

Equations for particle motion

To describe the particle motion correctly, one has to take into account all significant forces which act on particle during its motion. There are two kinds of such forces: those who act permamently, and those who act as impulses [7, 14, 20]. The source

for the first are presence of the gas phase and gravitation, an for the second particle-wall collisions, and particle-particle collisions.

Permament forces and torques

The most important is the drag force:

$$\vec{F}_D = \frac{1}{2}\rho\pi R^2 C_D(\vec{V}_g - \vec{V}_p)\left|\vec{V}_g - \vec{V}_p\right| \tag{7}$$

$$C_D = \frac{24}{\mathrm{Re}}, \qquad \mathrm{Re} < 0.2$$

$$C_D = \frac{24}{\mathrm{Re}}(1 + 0.1\,\mathrm{Re}^{0.99}) \qquad 0.2 < \mathrm{Re} < 2$$

$$C_D = \frac{24}{\mathrm{Re}}(1 + 0.11\,\mathrm{Re}^{0.81}) \qquad 2 < \mathrm{Re} < 21$$

$$C_D = \frac{24}{\mathrm{Re}}(1 + 0.189\,\mathrm{Re}^{0.632}) \qquad 21 < \mathrm{Re} < 200$$

$$C_D = \frac{24}{\mathrm{Re}}(1 + 0.15\,\mathrm{Re}^{0.687}) \qquad 200 < \mathrm{Re} < 1000$$

$$C_D = 0.44 \qquad 1000 < \mathrm{Re} < 2\cdot 10^5$$

$$C_D = 0.1 \qquad \mathrm{Re} > 10^5$$

$$\mathrm{Re} = \frac{2\rho R\left|\vec{V}_g - \vec{V}_p\right|}{\mu} \tag{8}$$

The second permanent force is gravitational force:

$$\vec{F}_g = m_p\vec{g} \tag{9}$$

Due to the frequent collisions with the walls in horizontal tubes and channels particles rotate with large angular velocity. This rotation in viscous fluid induce considerable lift force and torque, which have to be taken into account. Rubinow and Keller [15] analyzed rotation of the sphere in viscous fluids with small Reynolds numbers, and came to the relation:

$$\vec{F}_{Lr} = \pi R^3\rho\vec{\omega}\times\vec{V}[1 + O(\mathrm{Re})] \tag{10}$$

where $\vec{\omega}$ represents particle angular velocity, $\vec{V}$ velocity of sphere in fluid, and $O(\mathrm{Re})$ some function of the Reynolds number. As can be seen this force is perpendicular on particle velocity. It is the outcome of the change of the pressure field around the particle, due to its rotation. It is not function of viscosity. Viscosity appears in the expression for torque:

$$\vec{T} = -8\,\pi\mu\,R^3\vec{\omega}[1 + o(\mathrm{Re})] \tag{11}$$

It was shown in [15] that for low Re $O(\mathrm{Re})$ and $o(\mathrm{Re})$ can be neglected. It is now necessary to generalize these expressions for particle motion in turbulent flow. In that case the rotation of fluid should also be taken into account. This can be solved by introduction of one additional term $1/2\nabla\vec{V}_g$, [20]. Thus, we get:

$$\vec{F}_{Lr} = \pi R^3 \rho(\vec{\omega}_p - \frac{1}{2}\nabla\times\vec{V}_g)\times(\vec{V}_p - \vec{V}_g) \tag{12}$$

$$T = -8\pi\mu R^3(\vec{\omega}_p - \frac{1}{2}\nabla\times\vec{V}_g) \tag{13}$$

Rubinow and Keller also showed that particle rotation does not influence on drag force intensity, and vice versa. Therefore, they can be treated separately.

When particle is moved relatively to the fluid in which there is velocity gradient, there is no more symmetrical pressure field around the particle, and the resulting drag force deviates from the Stockes formula. This can be represented as the action of a new force (and drag force remains the same as before). This force is called Saffman force, and for small particles can be important in regions near the wall, where the fluid velocity gradients are high. This force was analyzed by Saffman [16], for the case of particle motion through very viscous fluid, and for the case of velocity gradient perpendicular to the direction of motion. Using the original Saffman's expression and generalizing it for the full three dimensional case, where fluid velocity gradient need not to be perpendicular to the vector of particle motion, one gets:

$$\vec{F}_{ls} = -1.5422\, m^p \frac{(\rho\mu)^{1/2}}{\rho^p d^p \left|\nabla\left|\vec{V}_p - \vec{V}_g\right|\right|^{1/2}} \nabla(\vec{V}_p - \vec{V}_g)^2 \tag{14}$$

In solving the equations of particle motion a semi-analytical approach was adopted. That means the following: the whole time interval was divided on subintervals, at the end of which particle position and velocity (angular velocity also) were calculated. During the particular time period it was assumed that values for lift and Saffman force do not change (for this assumption to be valid time intervals should be small enough). Now the basic equation:

$$\frac{d\vec{V}_p}{dt} = \frac{1}{\tau_p}(\vec{V}_g - \vec{V}_p) + \vec{g}\left[1 - \frac{\rho}{\rho_p}\right] + \frac{\vec{F}_{lr} + \vec{F}_{ls}}{m_p} \tag{15}$$

can be solved analytically, to get the following expressions for velocity components:

$$U_p = U_g - (U_g - U_{p0})\exp\left(-\frac{\Delta t}{\tau_p}\right) + \frac{3}{4}\frac{\rho}{\rho_p}\tau_p\left[1 - \exp\left(-\frac{\Delta t}{\tau_p}\right)\right]\cdot$$

$$\cdot\left\{\frac{F_{ls}}{m_p}\vec{i} + \left[(W_p - W_g)\left(\omega_{py} - \frac{1}{2}\left(\frac{\partial U_g}{\partial z} - \frac{\partial W_g}{\partial x}\right)\right)\right] - \right.$$

$$\left. -(V_p - V_g)\left(\omega_{pz} - \frac{1}{2}\left(\frac{\partial V_p}{\partial x} - \frac{\partial U_p}{\partial y}\right)\right)\right\} \tag{16}$$

$$V_p = V_g - (V_g - V_{p0})\exp\left(\frac{-\Delta t}{\tau_p}\right) + \frac{3}{4}\frac{\rho}{\rho_p}\tau_p\left[1-\exp\left(-\frac{\Delta t}{\tau_p}\right)\right]\cdot$$
$$\cdot\left\{\frac{\vec{F}_{is}}{m_p}\vec{j} - g\left(1-\frac{\rho}{\rho_p}\right) + \left[(U_p - U_g)\left(\omega_{pz} - \frac{1}{2}\left(\frac{\partial V_g}{\partial x} - \frac{\partial U_g}{\partial y}\right)\right) - \right.\right.$$
$$\left.\left. -(W_p - W_g)\left(\omega_{px} - \frac{1}{2}\left(\frac{\partial W_p}{\partial y} - \frac{\partial V_p}{\partial z}\right)\right)\right]\right\} \tag{17}$$

$$W_p = W_g - (W_g - W_{p0})\exp\left(-\frac{\Delta t}{\tau_p}\right) + \frac{3}{4}\frac{\rho}{\rho_p}\tau_p\left[1-\exp\left(-\frac{\Delta t}{\tau_p}\right)\right]\cdot$$
$$\cdot\left\{\frac{\vec{F}_{is}}{m_p}\vec{k} + \left[(V_p - V_g)\left(\omega_{px} - \frac{1}{2}\left(\frac{\partial W_g}{\partial y} - \frac{\partial V_g}{\partial z}\right)\right) - \right.\right.$$
$$\left.\left. -(U_p - U_g)\left(\omega_{py} - \frac{1}{2}\left(\frac{\partial U_p}{\partial z} - \frac{\partial W_p}{\partial x}\right)\right)\right]\right\} \tag{18}$$

Here, subscript '0' denotes the value at the beginning of time interval. For angular velocity:

$$\vec{\omega}_p = \frac{1}{2}\nabla\times\vec{V}_g + \left(\vec{\omega}_{p0} - \frac{1}{2}\nabla\times\vec{V}_{g0}\right)\exp\left(\frac{-15\mu}{\rho_p R^2}\Delta t\right) \tag{19}$$

Impulse forces

Particle-wall collision

The main question is how to model particle-wall collisions to get realistic results. For example, if we assume elastic collision, due to the absence of momentum loss, particle velocity will inevitably be approaching gas velocity. But in reality, gas and particle velocities always differ by some amount. Moreover, it is known that during the pneumatic conveying particles rotate with great angular velocity in the direction of their motion, which can not be take into account with elastic model. That means that restitution coefficient and friction coefficient must be included. It is also customary to treat particles as ideal spheres, and walls as smooth surfaces. But, with such assumptions (even if we include restitution and friction coefficients) due to the frequent collisions of particles with the wall in horizontal sections, particle vertical velocity component would be continually decreasing, with particle accumulation at the bottom wall as the outcome. But in praxis this does not happen. Gas turbulence and lift forces are not large enough to keep larger particles (over 100 μm in diameter) in the suspension. Therefore, the only mechanisms left are inter-particle and particle-wall collisions, where nonsphericity of particles and roughness of the wall were not neglected (or at least one of them). Influence

of nonsphericity is dominant for large particles, and decreases with the decrease of particle diameter. Quite contrary, influence of wall roughness increases with the decrease of particle diameter. Since this work treats transport of powders with mean diameter less than 200 μm, nonsphericity will be neglected, and particles would be treated as ideal spheres.

(a) Particle collision with the smooth wall

Basic assumptions of the model are:

(1) there are no fracture or plastic deformations of particles;
(2) there exists the period of particle sliding on the tube surface;
(3) when particle once stops to slide, it continues to roll along the whole period of contact with the surface;
(4) friction between the particle and the surface obeys Columb-s law;
(5) the curvature of the tube is in comparison to the particle diameter large enough for assumption that particle collides with the plane tangential to the tube surface at the point of collision.

The whole collision period can be divided on: (1) compression period (particle is elastically compressed); (2) recovery period (particle returns to the state before collision). Depending on when particle stops to slide, three types of collisions can be distinguished:

(I) particle stops to slide in the compression period,
(II) particle stops to slide in the recovery period,
(III) particle slides for the whole period of collision.

Which of these cases will happen depends on the friction factor f, restitution coefficient e, and the angle between particle velocity and the collision plane in the moment of collision. If we denote the direction of the main flow with x, and direction normal to the plane of the collision with y, we get the following conditions for each of these cases:

$$(1)\ \frac{V_y^{(0)}}{|V|} < -\frac{2}{7f} \quad (2)\ -\frac{2}{7f} < \frac{V_y^{(0)}}{|V|} < -\frac{2}{7f(1+e)} \quad (3)\ -\frac{2}{7f(1+e)} < \frac{V_y^{(0)}}{|V|} < 0$$

The expressions for the components of velocity and angular velocity are the same for the first two cases, and differs for the third. Therefore:

Cases (I) and (II):

$$V_x = \frac{5}{7}\left(V_x^{(0)} - \frac{2}{5}R\omega_z^{(0)}\right), \quad \omega_x = \frac{5}{7}\frac{1}{R}\left(V_z^{(0)} + \frac{2}{5}R\omega_x^{(0)}\right) = \frac{V_z}{R},$$

$$V_y = -eV_y^{(0)}, \qquad \omega_y = \omega_y^{(0)},$$

$$V_z = \frac{5}{7}\left(V_z^{(0)} + \frac{2}{5}R\omega_x^{(0)}\right), \quad \omega_z = -\frac{5}{7}\frac{1}{R}\left(V_x^{(0)} - \frac{2}{5}R\omega_z^{(0)}\right) = -\frac{V_x}{R} \qquad (20)$$

Case (III):

$$V_x = \varepsilon_x f(1+e)V_y^{(0)} + V_x, \quad \omega_x = -\frac{5}{2}\frac{\varepsilon_z f(1+e)V_y^{(0)}}{R} + \omega_x^{(0)},$$
$$V_y = -eV_y^{(0)}, \qquad \omega_y = \omega_y^{(0)}$$
$$V_z = \varepsilon_z f(1+e)V_y^{(0)} + V_z^{(0)}, \quad \omega_z = \frac{5}{2}\frac{\varepsilon_x f(1+e)V_y^{(0)}}{R} + \omega_z^{(0)} \tag{21}$$
$$\varepsilon_x = \frac{V_x^{(0)} + R\omega_z^{(0)}}{\sqrt{(V_x^{(0)} + R\omega_z^{(0)})^2 + (V_z^{(0)} - R\omega_z^{(0)})^2}}, \quad \varepsilon_z = \frac{V_z^{(0)} - R\omega_x^{(0)}}{\sqrt{(V_x^{(0)} + R\omega_z^{(0)})^2 + (V_z^{(0)} - R\omega_x^{(0)})^2}}$$

It was taken that the restitution coefficient $e = 0.97$ and friction factor $f = 0.8$.

(b) Modeling of roughness

Roughness of tubes are in real plants very important, especially for small particles. Due to the fact that the horizontal particle velocity component is much larger than the vertical one, even a small roughness may induce considerable change in the vertical momentum. So, the collisions of particles with the rough wall can become the dominant mechanism in keeping the solid phase in suspension in horizontal parts of the pneumatic conveying system.

Roughness can be modeled on several ways. In some works smooth wall was replaced with some periodic function. It is usually sinusoidal function, Matsumoto and Saito [12], whose amplitude and period are some characteristic roughness parameters. The main disadvantage of such models lays in the fact that on this way roughness become strictly regular, although it is stochastic in nature, due to the large number of noncorrelating influences during the tube manufacturing.

In this work the roughness was modeled by replacing the real plane of collision by virtual plane which inclines in the direction of particle motion (Fig. 1). This method was first used by Tsuji [10, 11]. That actually means that we change the angle of particle velocity in the moment of collision. The term virtual emphasizes the fact that we neither deal with the real inclination of the wall nor with the change of flow domain geometry, so for the other part of the model the previous, real wall is relevant. The angle of inclination is not constant parameter. One value is valid only for one particle, and only

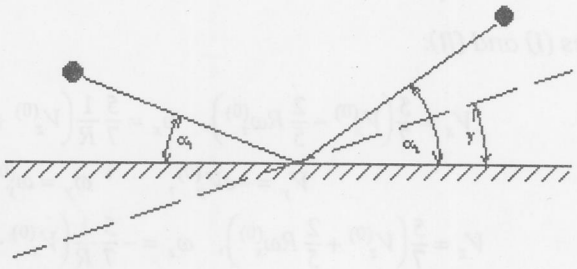

Figure 1. Replacement of real wall by virtual one (dashed line) to simulate wall roughness

for one collision. In order to retain the stochastic nature of roughness in reality, its value was also assumed to be stochastic.

To model the three-dimensionallity of the roughness, an angle which turns the collision plane about the vertical axis was introduced. So, the basic features of the model are:

(1) The position of virtual plane is determined by two angles, γ and δ. γ determines the angle of inclination of the virtual plane from the real one, and δ the position of virtual plane related to the direction of main flow;

(2) Both angles are stochastic parameters, generated in the model randomly. The density distribution is Gaussian:

$$\rho(\gamma) = \frac{1}{\overline{\Delta\gamma}\sqrt{2\pi}} \exp\left(-\frac{(\gamma-\bar{\gamma})^2}{2\overline{\Delta\gamma}^2}\right), \qquad \overline{\Delta\gamma} = (\overline{\gamma^2})^{1/2}, \qquad \bar{\gamma} = 0 \tag{22}$$

Since the mean value of Gaussian distribution is zero, the angle can take both positive and negative values with the same probability. Although the domain of the Gaussian distribution is $-\infty < \gamma < +\infty$, due to the determined value of standard deviation (see below) in practice γ can not exceed more than few degrees. The domain of δ is $-\pi/2 < \delta < \pi/2$. From the unisotropity of roughness follows the uniform distribution for δ.

(3) Particle coordinate does not depend on the values of mentioned angles. That is, it was not supposed that roughness affects tube diameter. It follows that the particle velocity at the moment of impact is the same as in the model without roughness.

The basis for determination of $\overline{\Delta\gamma}$ was work of Frank and Petrak [9], who analyzed the influence of the relative sizes of roughness and particle diameters on the type of collision, and gave the expressions for the maximal value z_{max} of the roughness height (see Fig. 2):

$$(1)\ 2R < \overline{E_R} + \frac{1}{4}\frac{\overline{E_A}^2}{\overline{E_R}} \Rightarrow z_{max} = \frac{1}{2}\overline{E_A}\frac{\sqrt{\overline{E_R}/2R}}{\sqrt{1-\overline{E_R}/2R}} \tag{23}$$

$$(2)\ \overline{E_R} + \frac{1}{4}\frac{\overline{E_A}^2}{\overline{E_R}} < 2R < \frac{\overline{E_A}^2 + \overline{\Delta E_R}^2}{\overline{\Delta E_R}} \Rightarrow z_{max} = \frac{1}{2}\overline{E_A}\tan\gamma$$

$$\gamma = \frac{1}{2}\left(\arcsin\left(\frac{\sqrt{\overline{\Delta E_R}^2 + \overline{E_A}^2}}{2R}\right) + \operatorname{arctg}\left(\frac{\overline{\Delta E_R}}{\overline{E_A}}\right)\right) \tag{24}$$

$$(3)\ \frac{\overline{E_A}^2 + \overline{\Delta E_R}^2}{\overline{\Delta E_R}} < 2R \Rightarrow z_{max} = \frac{1}{2}\overline{E_A}\frac{\sqrt{\overline{\Delta E_R}/2R}}{\sqrt{1-\overline{\Delta E_R}/2R}} \tag{25}$$

It was assumed that to z_{max} correspond the value γ_{max} of the largest angle of inclination. According to the statistical rule 3σ, this is the triple value of standard deviation, therefore:

$$\overline{\Delta\gamma} = \frac{1}{3}\gamma_{\max} = \frac{1}{3}\operatorname{arctg}\left(\frac{z_{\max}}{E_A}\right)$$

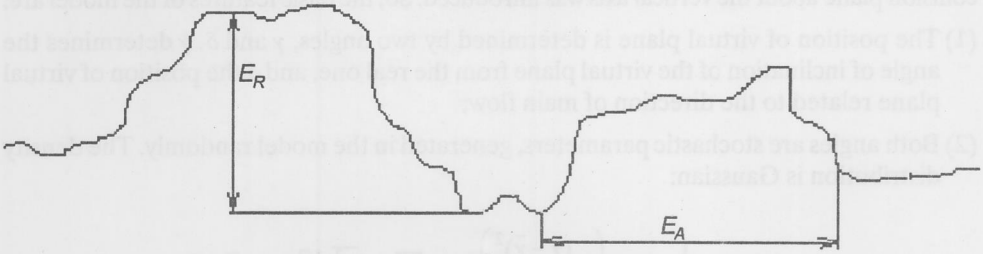

Figure 2. Deffinition of the characteristics of roughness, E_R and E_A

Particle radius distribution and notion of the parcel

Powder materials are polydispersed. In horizontal sections of pneumatic conveying systems the influence of particle size on dense phase concentration profile is so great that this fact has to be taken into account. For particle radius the log-normal distribution was assumed, since Sommerfeld [6] showed that this gives the best agreement of numerical results with experiment:

$$f(R) = \frac{1}{\sqrt{2\pi\sigma^2}\,R}\exp\left(-\frac{(\ln R - \ln R_m)^2}{2\sigma^2}\right), \qquad \sigma^2 = \ln\frac{R_m}{R_{N\max}} \tag{26}$$

where R_m and $R_{N\max}$ are mean and the most probable radius, respectively. σ depends on the particular ensemble of particles. In this work it was taken that $\sigma^2 = 0.18$.

The deficiency of Lagrangian approach is that the number of particles present in the flow domain is enormous. In modeling one must confine himself to follow only a moderate number of them. On this way we are coming to the notion of "parcels". They are particles we follow in our model. Each of them represents a large bulk of real particles with the same characteristics (size, velocity, ...).

Now it is necessary to derive the particle size distribution. It is different from log-normal distribution due to the way of dispersed phase feeding into the system. It is performing by generating parcels at the entrance in regular time intervals. With the assumption of continuous and stationary feeding, the same mass equivalent are assigned to each parcel. Since different parcels have different diameters, every parcel represents different number of particles in the flow domain. Since we are interested to get the

log-normal distribution for the ensemble of all particles (and not for the ensemble of parcels) for the distribution of parcel radius, one gets the following expression, [6]:

$$g(R) = \frac{4\pi\rho R^2}{3m_p\sqrt{2\pi\sigma^2}} \exp\left(-\frac{(\ln R - \ln R_m)^2}{2\sigma^2}\right) \tag{27}$$

Particle-particle collision

Under certain conditions particle-particle collisions can have great influence on the fields of dispersed phase parameters. They induce: (1) momentum transfer between particles; (2) kinetic energy dissipation; (3) change of the shape, or even splitting the particles; (4) accumulation. Their importance is determined by the their frequency, which means that they should be taken into account in the cases of: (1) relatively large volume loading ratio between dispersed and the gas phase; (2) great intensity of particles velocity fluctuations, relating to their mean velocity.

Due to the enormous number of particles in the flow domain, it is impossible to look for the possible interaction between any pair. Instead, the stochastic approach has been chosen. Its basic features are:

(1) for the particle which is followed (parcel) the probability of collision with any other particle in the domain in the given time interval is calculated;
(2) the collision of the followed particle is considered to be a stochastic event, to which the probability calculated in (1) is corresponded;
(3) collision influences only the followed particle. The other participant of the collision is only the cause of the collision, and is therefore a virtual particle. On this way parcels were completely detached from each other, and due to the Lagrangian approach are treated separately. The field characteristics of the dispersed phase are included in the model over the velocity and size of virtual particles;
(4) particles are smooth (there is no friction between the surfaces of the particles in collision), therefore collisions do not affect their angular velocities.

The model is based on the fact that due to the enormous number of particles, their collisions can be treated very similarly as molecular collisions are treated in the kinetic theory of gases. The condition for local quasistationarity of dispersed phase is fulfilled with the assumption of considering the system in stationary state, and large number of particles per unit volume.

The whole procedure consists of three steps:

(1) calculation of the fields of parameters which are neccesary to calculate collision probability (*i. e.* particle mean velocities and concentration);
(2) calculation of the collision probability;
(3) application of the stochastic collision model.

Sommerfeld and Živković showed in [22] that for usual flow conditions and time step $\Delta t \sim 1 \cdot 10^{-3}$ s in which the probability of the collision of the followed particle with some other particle was calculated, the followed particle will collide mostly once (error

made on that way is less than 1%). They also showed that in the case of isotropic turbulence with high dissipation rate (where particles do not follow fluid stream lines) the following expression for probability of collision can be derived:

$$Z_{1k} = \frac{N_1 N_k \Delta t}{8\pi^2 V_k (\overline{V_1^2 V_k^2})} \int_0^\infty f(R_2)(R_1+R_2)^2 dR_2 \int\int_{-\infty}^{\infty} \int\int\int \left[(V_{11}-V_{12})^2 + (V_{21}-V_{22})^2 + (V_{31}-V_{32})^2\right]^{1/2} \exp\left(-\frac{V_{i1}V_{i1}}{2\overline{V_1^2}} - \frac{V_{i2}V_{i2}}{2\overline{V_2^2}}\right) dV_{11}dV_{12}dV_{13}dV_{21}dV_{22}dV_{23}$$

$$P_{col} = \frac{Z_{1k}}{N_1} = \frac{2^{3/2}\pi^{1/2} N_k \Delta t}{V_k}\left(R_1^2 + 2R_1 \frac{R_m^{3/2}}{R_{Nm}^{1/2}} + \frac{R_m^4}{R_{Nm}^2}\right)\sqrt{\overline{V_1^2} + \overline{V_k^2}} \qquad (28)$$

Here, Z_{1k} represents the total number of collisions of one particular set of particles with same characteristics, (size, velocity, *etc.*) and the set of all particles in control volume. $f(R_2)$ represents assumed particle distribution. It was also assumed that in one control volume the Gaussian distribution of particle velocities exists. $\overline{V_k^2}$ is statistical characteristics of the whole ensemble, and can be calculated on the basis of dispersed phase velocity field.

On the basis of calculated probability, it is randomly chosen whether the collision would happen. If the answer is positive, the position, size and velocity of virtual particle are generated randomly, too. Problem of the position generation lies in the fact that due to the motion of parcel, virtual particle will not hit the parcel at every point with the same probability. To overcome this difficulty one should look the collision in the coordinate system which travels with the virtual particle. In it, collision can happen only at some point of the front half of the surface of parcel.

From Fig. 3. it is obvious that the collision domain (volume in which the center of virtual particle has to be placed for collision to happen) represents a cylinder around

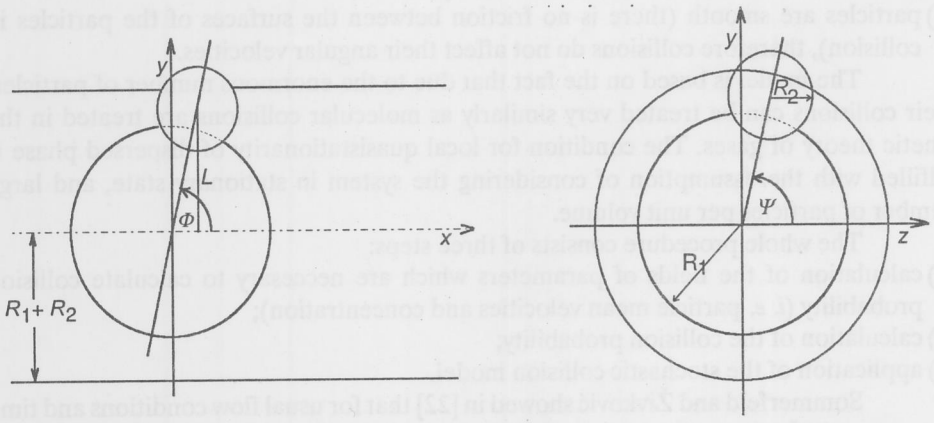

Figure 3. Collision domain

the parcel, with the diameter equal to the sum of diameters of parcel and virtual particle. Control volume dimensions are by definition small enough to fulfill the condition of the same characteristics of dispersed phase on its whole domain. Therefore, the probability for virtual particle to be found in any point of the cylinder is the same, and it is also worth for points in any cross-section of the cylinder (that of course does not mean that the collision probability distribution over the surface of the front half-sphere is uniform). The position of the center of the virtual particle related to cylinder axis is determined by sampling two stochastic parameters (x and y), with uniform distribution in the domain $0 < x, y < R_1 + R_2$ (Fig. 4). If the sampled position is found outside the cylinder (shadowed surface), x and y are generated again. Now, one gets:

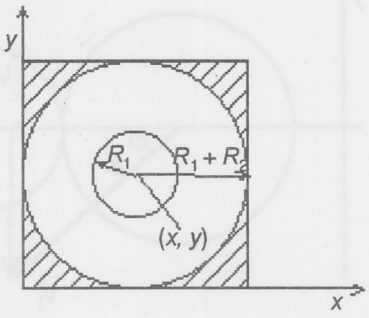

Figure 4. The domain for sampling the position of the center of the virtual particle

$$L = \sqrt{x^2 + y^2}, \quad \Phi = \arcsin\left(\frac{L}{R_1 + R_2}\right) \tag{29}$$

For the full determination of virtual particle position it is also necessary to have angle Ψ. It is got by sampling of random number with uniform distribution in the domain $0 < \Psi < 2\pi$.

To get the collision equations in the simplest form, it is necessary to change reference system. Beside the already mentioned transformation to the system of reference which travels together with the virtual particle, three additional rotations of that system are necessary:

(1) transformation to the system in which the parcel velocity is collinear with some of the coordinate axis (say x);

(2) transformation to the system in which the plane defined by the vector of particle velocity and the line which connects the centers of parcel and virtual particle coincide with some of the coordinate planes (say $x - y$);

(3) transformation to the system in which the line which connects the centers of parcel and virtual particle coincide with one of the axis in coordinate plane chosen in (2). The picture of collision in this final system of reference is shown on Fig. 5.

Now, for the new parcel velocity components after the collision one gets:

$$V'_{1x} = V_{1x}\left(1 - \frac{1+k}{1+\frac{R_1^{1/3}}{R_2^{1/3}}}\right), \quad V'_{1y} = V_{1y} \tag{30}$$

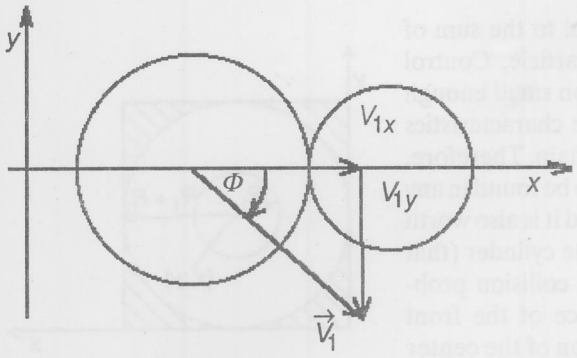

Figure 5. Particle collision in final system of reference

where k represents restitution coefficient. In the calculation in this work it was assumed $k = 1$.

To get the desired parcel velocity in system of reference attached to the tube, the inverse coordinate transformation to those mentioned above are necessary, in the inverse order, of course.

The change of particle angular velocity due to particle-particle collisions was not taken into account.

It is obvious that in one flow domain particle collisions will occur no matter how dilute the mixture actually is. But their importance grow with their number per unit volume and unit time. Since the modeling of particle-particle collisions consumes a lot of mathematical effort, it is desirable to derive a criteria for its inclusion in the model. That means, (although on that way some little mistake will be done) in the course of saving computational time, in cases where they are not important, particle-particle collisions will be neglected.

In so called dilute flow, particle velocity is governed by aerodynamic and body forces. In so called dense flow particle collisions control particle velocity. The influence of the collision on particle motion can be evaluated by comparing mean time between collisions τ_c with the aerodynamic responce time τ_A. In [18] Crowe defined dilute flow when $\tau_A/\tau_c < 1$, and opposite, dense flow when $\tau_A/\tau_c > 1$. Here:

$$\tau_A = \frac{2}{9}\frac{\rho_p R^2}{f\mu}, \quad f = \frac{\mathrm{Re}\, C_D}{24} \tag{31}$$

Now, it is reasonably to assume the same criterion for inclusion of particle-particle collisions into the model. Namely, inter-particle collisions will be included in dense flow, when $\overline{\tau_A / \tau_c} > 1$. The time between two collisions of one particle with other particles is reciprocal value of the collision frequency. Therefore, for the ensemble 1 of particles of the same type:

$$\left(\frac{1}{\tau_c}\right)_1 = \frac{Z_1}{N_1 \Delta t} = \frac{2^{3/2}\pi^{1/2} N}{V}\left(R_1^2 + 2R_1\frac{R_m^{3/2}}{R_{Nm}^{1/2}} + \frac{R_m^4}{R_{Nm}^2}\right)\sqrt{\overline{V_1^2} + \overline{V^2}} \tag{32}$$

and using expression (31):

$$\left(\frac{\tau_A}{\tau_c}\right)_1 = \frac{2^{5/2}\pi^{1/2}\rho_p N}{9f\mu V}\left(R_1^4 + 2R_1^3\frac{R_m^{3/2}}{R_{Nm}^{1/2}} + R_1^2\frac{R_m^4}{R_{Nm}^2}\right)\sqrt{\overline{V_1^2}+\overline{V^2}} \tag{33}$$

The ratio N/V is given by the following relation:

$$\frac{N}{V} = \frac{3M_l\rho}{4\pi\rho_p\int_0^\infty f(R)R^3dR} = \frac{3M_l\rho}{4\pi\rho_p\int_0^\infty \frac{R^2}{\sqrt{2\pi\sigma^2}}\exp\left(-\frac{(\ln R-\ln R_m)^2}{2\sigma^2}\right)dR} = \frac{3M_l\rho R_{N\max}^{9/2}}{4\pi\rho_p R_m^{15/2}}$$

where M_l represents particle to gas mass loading ratio. Now, it remains to perform averaging over the whole set of particles. On the first sight diameter averaging looks natural. But, on that way it can happen that the most dominant influence on the value of calculated criterion perform those fractions (with small diameter and hence small mass) whose mass is small or negligible comparing with the total mass of dispersed phase. For that reason the mass averaging of the expression (33) was performed:

$$\overline{\left(\frac{\tau_A}{\tau_c}\right)} = \frac{\int_0^\infty f(R_1)R_1^3\left(\frac{\tau_p}{\tau_c}\right)_1 dR}{\int_0^\infty f(R_1)R_1^3 dR} = \frac{2M_l\rho}{3f\mu\pi^{1/2}}\sqrt{\overline{V^2}}R_m\left(\frac{R_m^{31/2}}{R_{N\max}^{31/2}} + 2\frac{R_m^{19/2}}{R_{N\max}^{19/2}} + \frac{R_m^{11/2}}{R_{N\max}^{11/2}}\right) \tag{34}$$

Numerical models and results

For getting the numerical solution of gas equations control volume method was adopted. Since the full 3-D model was developed, it was not possible to take staggered grid for velocity components. Instead, the algorithm with collocated grid and hybrid scheme was developed. The basis for it was CAST algorithm for single phase flow.

Three different geometries were calculated: (1) horizontal plain channel; (2) horizontal circular tube; (3) combination of horizontal tube, 90° bend, and vertical tube:

(1) For this geometry the results have been already presented in [22]. They were repeated here in order to get a full insight on all properties of the model. In this case 2-D model was used, and the influence of the side walls was neglected. Channels were 6.5 m long. Influence of roughness was analyzed on 26 mm high channel, and for this geometry particle-particle collisions were not taken into account. The influence of particle-particle collision on concentration profile was analyzed on 100 mm high channel. Mean gas velocities were 7 and 10.7 m/s. Particle diameters were 40, 100 and 500 μm, with density ρ = 2500 kg/m^3. Some results can be seen on the Figures 6–9. Channel height has been divided on seven sections, and normalized mass flux in every section represents mass flux at this section, divided by total mass flux in that cross section. From Figs. 6 and 7 can be seen that irregular bouncing play important role in keeping particles in

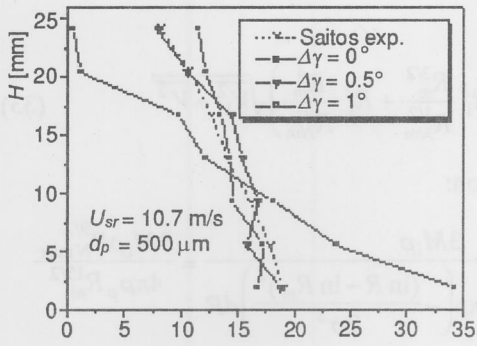

Figure 6. Normalized mass flux at the outlet of the plane channel

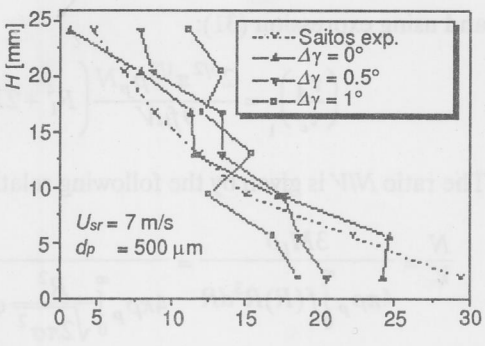

Figure 7. Normalized mass flux at the outlet of the plane channel

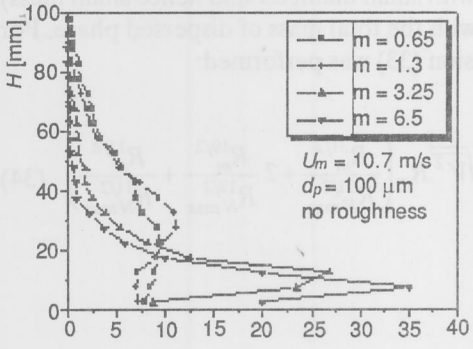

Figure 8. Normalized mass flux at the outlet of the plane channel

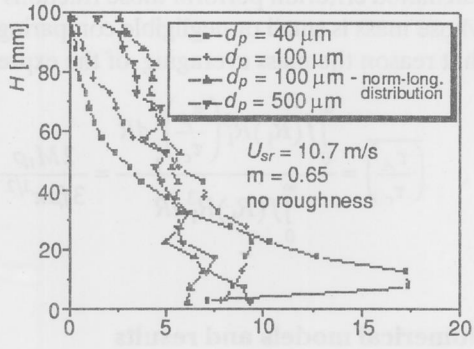

Figure 9. Normalized mass flux at the outlet of the plane channel

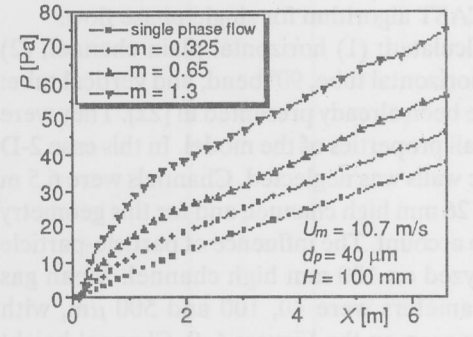

Figure 10. Pressure distribution along the pipe due to the presence of dispersed phase

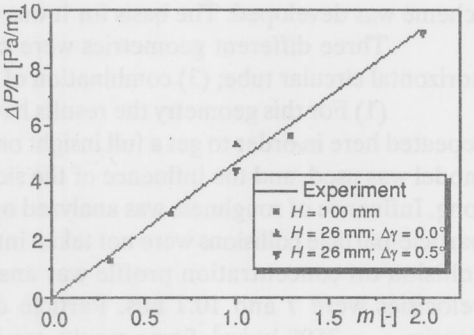

Figure 11. Comparison of experimental and computational specific pressure drop

suspension. Fig. 8 and Fig. 9 show the influence of particle/gas mass loading ratio and particle diameter on profile of particle mass flux. On Fig.10. the additional pressure drop due to the presence of dispersed phase was presented. It can be seen that greater particle to gas mass loading ratio induce greater pressure drop per unit length. This is mainly due to the fact that in collision with the rough wall particles loose a considerable part of its axial velocity, which has to be compensated with gas pressure energy. Also, greater roughness induce greater pressure drop, since greater roughness induce larger transfer of horizontal particle velocity component into vertical component during the collision process. Comparison of calculated pressure drop per unit length with experimental results is given on Fig. 11.

(2) Due to the presence of gravity, computation of flow in horizontal circular tubes needs a full 3-D code. Tube diameter was 80 mm, and its length 6 m. Computation were performed for several velocities, roughness and mass loadings. Particle mean diameter was 40 μm. Some results of calculated normalized mass flux (this time tube was divided in ten sections), were presented on Fig. 12. Position zero means the bottom of

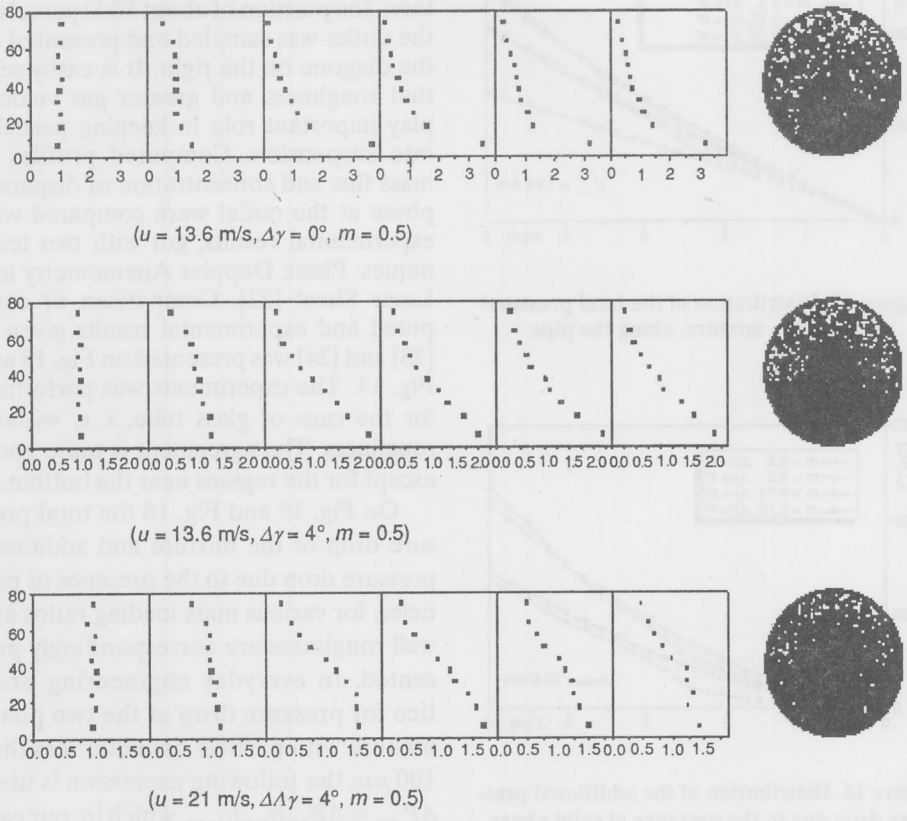

Figure 12. Normalized mass flux of dispersed phase

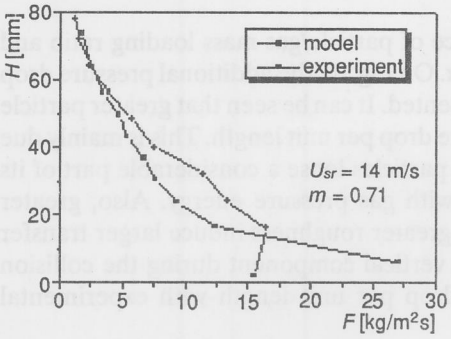

Figure 13. Distribution of particle mass flux

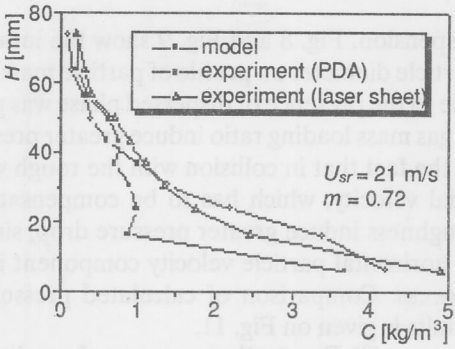

Figure 14. Distribution of particle mass flux

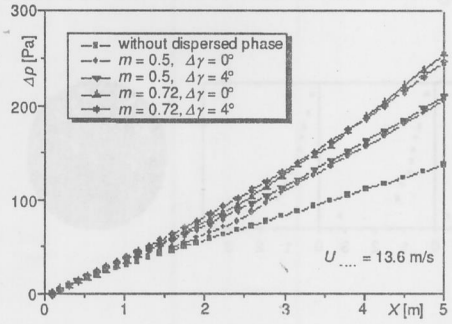

Figure 15. Distribution of the total pressure drop of the mixture, along the pipe

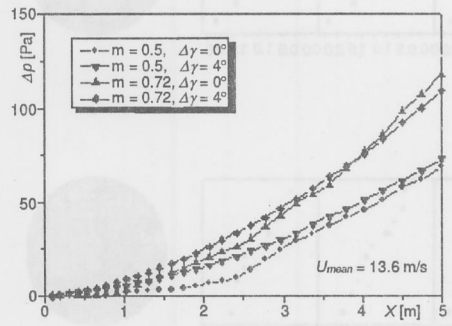

Figure 16. Distribution of the additional pressure drop due to the presence of solid phase, along the pipe

the tube. Results are given in six different cross sections, after every 1m of distance in axial direction. To get an intuitive picture, the position of about 5000 parcels at the outlet was sampled and presented on the diagram on the right. It is easily seen that roughness and greater gas velocity play important role in keeping particles into suspension. Computed profiles of mass flux and concentration of dispersed phase at the outlet were compared with experimental results, got with two techniques: Phase Doppler Anemometry and Laser Sheet [22]. Comparison of computed and experimental results given in [23] and [24] was presented on Fig. 13 and Fig. 14. The experiments was performed for the case of glass tube, *i. e.* without roughness. The agreement is quite good, except for the regions near the bottom.

On Fig. 15 and Fig. 16 the total pressure drop of the mixture and additional pressure drop due to the presence of particles, for various mass loading ratios and wall roughness are correspondingly presented. In everyday engineering practice for pressure drop of the two phase mixture with particle diameter less than 100 μm the following expression is used: $\Delta P_{mix} = \Delta P_{gas}\rho_{mix}/\rho_{gas}$, which in our case means: $\Delta P_{mix} = \Delta P_{gas}(1 + m)$. For cal-

culation of ΔP_{gas} the Blasius expression for friction factor was used: $\zeta = 0.316/\mathrm{Re}^{0.25}$. This led to the idea that for pressure drop calculation the two-phase mixture can be treated as single-phase fluid with $\rho_{gas} = \rho_{mix}$, in other words, to include the density of mixture directly into the equations of flow (instead of multiplying the result of pressure drop for single-phase fluid with the correction factor due to the presence of the other phase). The results for two mass loading ratios are presented on Figs. 17 and 18. It can be seen that the mere change of density is not enough to compensate the presence of the other phase. This can be explained with the fact that density change causes the change of Reynolds number in the Blasius expression. Therefore, fluid viscosity has to be also multiplied with the mass loading ratio, to prevent the change of Reynolds number. For the gas parameters defined on that way, the excellent agreement with two-phase model and Blasius expression was got.

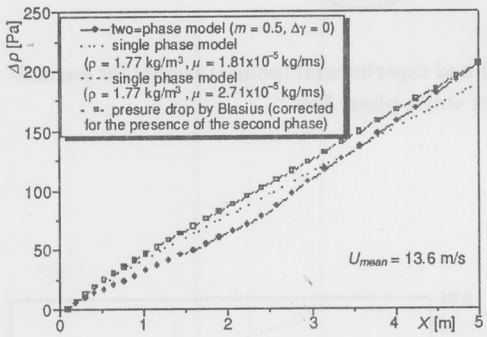

Figure 17. Compariosn of presure drop for two-phase and modified single phase flow

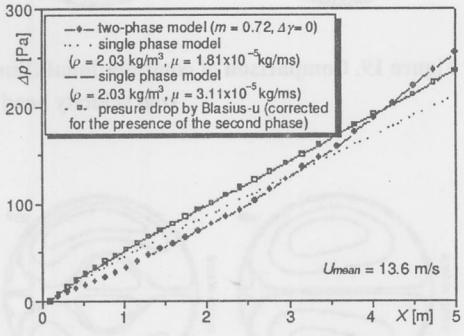

Figure 18. Compariosn of presure drop for two-phase and modified single phase flow

(3) The single phase model for flow in the bend was checked on the geometry which consisted only of bend of 180°. Radius of the tube was 0.1 m, and curvature of the bend 2.4 m. A developed flow at the entrance was assumed, with velocity at the center v_c = 21.3 m/s, so that Re = $2.36 \cdot 10^5$. The results were compared with experimental results of [19]. On Fig. 19 both computational (solid lines) and experimental (points) results for normalized velocity head ($\rho_u^2/\rho U_0^2$) in seven different cross-sections were presented. Relatively good agreement was got (especially when one has in mind that the squares of velocities were compared, so the velocities are much more closer to each other). For flow in curved tubes it is characteristic the existence of so called 'secondary flow', *i. e.* the flow in the cross section perpendicular to the main flow. Flow pattern of secondary flow for characteristic cross-sections were presented on Fig. 20.

For two-phase flow tube radius was 25 mm, and the bend radius of 90° bend was 500 mm (R/D = 10). Length of the straight sections was 2 m. Two different positions were

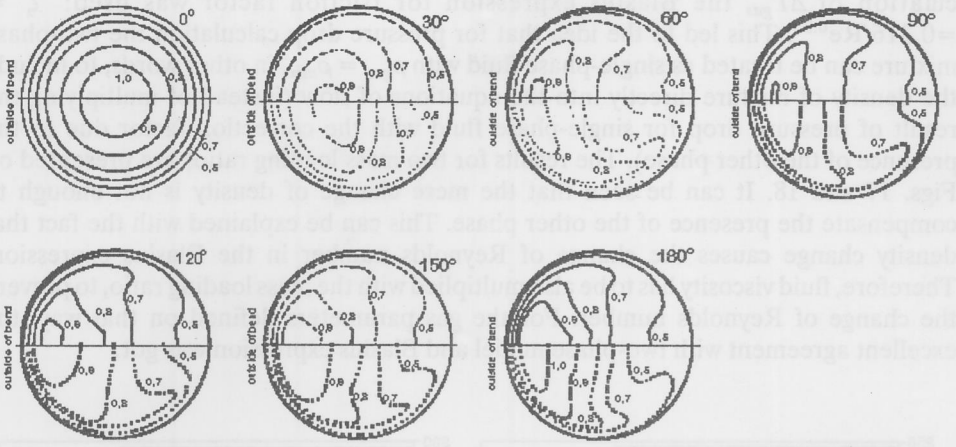

Figure 19. Comparison of computational (lines) and experimental (points) results for normalized velocity head for single phase flow

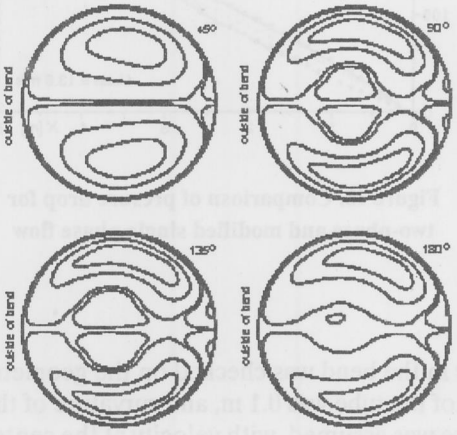

Figure 20. Secondary flow in single phase flow

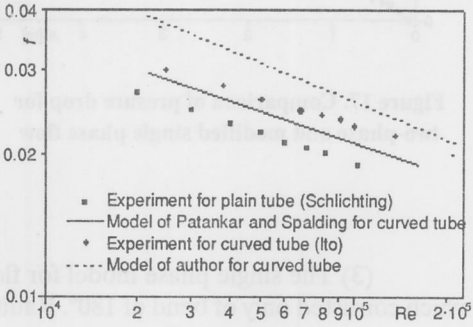

Figure 21. Comparison of computed pressure drop for single phase flow with experiments

considered: (a) bend lies in vertical plane (first straight section is horizontal, and the second vertical, with mixture going upward); (b) bend lies in horizontal plane. Results for normalized mass flux profiles were given on Fig. 22. Particle density was 923 kg/m^3, and their mean diameter 40 μm. In all cases the mean velocity of the main flow was 20 m/s. Presented cross-sections are: (1) entrance; (2) end of the first straight section; 3)

middle of the bend (α = 450°); (4) end of bend; (5) end of the second straight part (exit of the pipeline).

The comparison of the results for pressure drop got in single phase model with experimental results for plain and curved tube, as well as with numerical results of Patankar and Spalding are presented on Fig. 21. Pressure drop was expressed over the friction coefficient, and given in dependence of Re. It can be seen that curvature causes the enlargement of pressure drop, but this influence is greater than it was found in experiments of Ito [21]. The numerical results of Patankar and Spalding [17] are somewhat closer to the experiment, but it is placed on the other side of it.

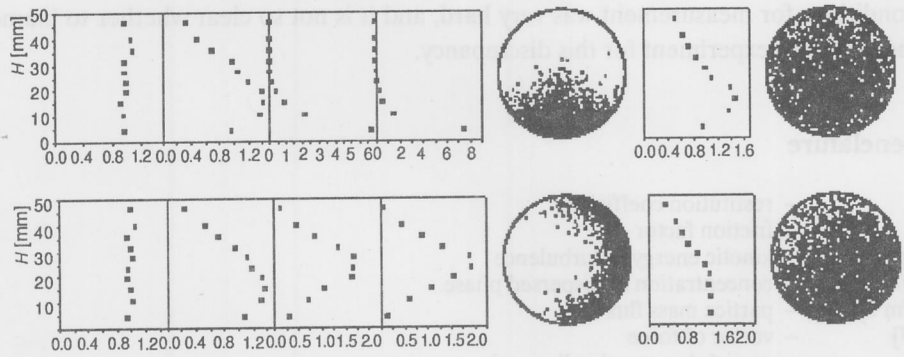

Figure 22. Nosmalized mass flux of dispersed phase in pipe with 90° bend

Conclusion

This work is a part of comprehensive research in the field of mathematical modeling of two phase flow of gas and dispersed phase. It is based on earlier models, which modeled gas phase rather well, as well as coupling the phases, heat and mass transfer in gas phase, chemical reactions. On the other side, the basic deficiency of these models was neglecting of some effects in the modeling of dispersed phase, such as particle-wall and particle-particle interactions, which can considerably influence two-phase pattern in some plants (like pneumatic conveying pipelines). Turbulence, as well as vast number of mutually interacting particles give to this type of flow clearly stochastic nature. In the development of the model it was persisted on it. On this way it was evaded the inclusion of some empirical or semi empirical parameters, as for example dispersed phase diffusion velocity. Such approach enables further developing of the model for more complex types of flow including chemical and thermal processes, where the particle motion is only one of the phenomena in consideration, and where is not so clear how to modify these empirical parameters to get satisfying solution. On the other side such approach has deficiency that the computer consumption time is much larger.

The most significant results of computation are particle concentration and velocity fields, as well as additional pressure drop due to the presence of particles. It was concluded that particle-particle and particle wall collisions play dominant role in keeping particles into suspension, and preventing sedimentation at the bottom. With increasing the particle mass loading, the concentration profile becomes more uniform at intermediate loadings. But at very high loadings the redistribution of the particles is hindered due to the increasing number of particle-particle collisions and decreasing the particles' mean free path. Roughness of the wall are found to be very important also. The comparison with numerical results are relatively good, except at the very vicinity of the bottom of the tube. But due to the high concentration of dispersed phase in that region the conditions for measurement was very hard, and it is not so clear whether to blame the model or the experiment for this discrepancy.

Nomenclature

e – restitution coefficient
f – friction factor
k [J/kg] – kinetic energy of turbulence
C [kg/m^3] – concentration of dispersed phase
F [kg/m^{2}s] – partice mass flux
$\vec{F}$ [N] – vector of force
m – particle/gas mas loading ratio
R [m] – radius of the particle
Re – Reynolds number
S_i^p [kg/m^{2}s^2] – momentum source terms due to the presence of particles
S_k^p [J/m^{3}s] – turbulent energy source term due to the presence of particles
S_ε^p [J/m^{3}s^2] – energy dissipation source term due to the presence of particles
$\vec{U}$ [m/s] – mean velocity in vector notation
$\vec{V}_g, \vec{V}_p$ [m/s] – vectors of gas and particle velocities
ε [m^2/s^3] – turbulent energy dissipation
μ, μ_t, μ_{ef} [Pa s] – viscosity, turbulent viscosity, effective viscosity
ρ [kg/m3] – density
τ_A [s] – aerodynamic response time
τ_c [s] – mean time between the collisions of some particle with any other particle
ω [rad/s] – angular velocity

References

[1] Patankar, S. V., Nunerical Heat Transfer and Fluid Flow, Hemisphere publ. Co., New York, 1980
[2] Hinze, J.O., Turbulence, 2nd Edition, Mc-Graw-Hill, New York, 1975
[3] Launder, B.E., Spalding, D.B., The Numerical Computation of Turbulent Flows, Computer Methods in Applied Mechanics and Engineering, *3*, pp. 269–289, 1974
[4] Lee, S. L., Durst, F., On the Motion of Particles in Turbulent Duct Flows, *Int. J. Multiphase Flow, 8*, (1982), pp.125–146
[5] Crowe, C. T., Sharma, M. P., Stock,D. E., The Particle-Source-in-Cell (PSI-CELL) Model for Gas-Droplet Flows, *Journal of Fluids Engineering*, June 1977

[6] Sommerfeld, M., Expansion of a Gas-Particle Mixture in a Supersonic Free Jet Flow, Z. für Flugwiss. und Weltraumforschung, *11* (1987), pp. 87–96
[7] Durst, F., Raszillier, H., Analysis of Particle-Wall Interaction, *Chemical Engineering Science,* 4 (1989), 12, pp. 2872–2879
[8] Durst, F., Milojević, D., Schonung, B., Eulerian and Lagrangian Predictions of Particulate Two-Phase Flows: a Numerical study, Applied Mathematical Modelling, *8*, pp. 101–115, April, 1984
[9] Frank, T., Petrak, D., Computersimulation der feststoffbeladenen Gasströmung im horizontalen Kanal mit Hilfe des Lagrange-Modells unter Berücksichtigung von Wandrauhigkeiten, Institut für Mechanik der AdW der DDR Karl-Marx-Stadt
[10] Tsuji, Y., Shen, N. J., Morikawa, Y., Numerical Simulation of Gas-Solid Flows. I - Particle-to-Wall Collision, Technology Reports of the Osaka University, *39*, No.1975, pp. 233–241, October 1989, Osaka, Japan
[11] Tsuji, Y., Shen, N. J., Morikawa, Y., Numerical Simulation of Gas-Solid Flows. I - Calculation of a Two-Dimensional Horizontal Channel Flow, Technology Reports of the Osaka University, *39*, No.1976, pp. 243-254, October 1989, Osaka, Japan
[12] Matsumoto, S., Saito, S., Monte Carlo Simulation of Horizontal Pneumatic Conveying Based on the Rough Wall Model, *Journal of Chemical Engineering* of Japan,*3* (1970), 2, pp. 223–230
[13] Milojević, D., Lagrangian Stochastic-Deterministic (LSD) Predictions of Particle Dispersion in Turbulence, Part. Part Syst. Charact., *7*, pp. 181–190, 1990
[14] Oesterle, B., Petitjean, A., Simulation of Particle-to-Particle Interactions in Gas-Solid Flows, *Int. J. Multiphase Flow, 19* (1993), 1, pp. 199–211
[15] Rubinow, S. I., J. Keller, B., The Transverse Force on a Spining Sphere Moving in a Viscous Fluid, *Journal of Fluid Mechanics, 11*(1961), pp. 447–459
[16] Saffman, P. G., The Lift on a Small Sphere in a Shear Flow, *Journal of Fluid Mechanics, 22* (1965), Part 2, pp. 385–400
[17] Patankar, S.V., Spalding, D. B., A Calculation Procedure for Heat, Mass and Momentum Transfer in Three-Dimensional Parabolic Flow, *Int. Journal of Heat and Mass Transfer, 15* (1972), pp. 1787–1806
[18] Crowe, C. T., On the Relative Importance of Particle-Particle Collisions in Gas-Particle Flows, IMechE, C78, pp. 135–137, 1981
[19] Rowe, V. M., Some Secondary Flow Problems in Fluid Dynamics, Ph.D. thesis, Cambridge University, 1966.
[20] Ahmad, K., Goulas, A., A Numerical Study of the Motion of a Single Particle in a Duct Flow, Fifth International Conference on the Pneumatic Transport of Solids in Pipes, April 16–18, London 1980
[21] Ito, H., Friction Factors for Turbulent Flow in Curved Pipes, Trans. ASME, *J. Basic Engineering*, *82* (1959), pp. 123–132
[22] Sommerfeld, M., Živković, G., Recent Advances in the Numerical Simulation of Pneumatic Conveying Through Pipe Systems, Computational Methods in Applied Sciences, 1992, pp. 201–212
[23] Huber, N., Sommerfeld, M., Digital Image of Laser Sheet Visualizations; an Effective Method to Characterize the Nonuniformity of Two-Phase Flows, ICHMT Seminar on Imaging in Transport Processes, May 25–29, 1992, Athens
[24] Sommerfeld, M., Živković, G., Huber, N., Optimization of Pneumatic Conveying of Coal Dust in Pipe Systems with the Regard to an Efficient Combustion with Low Polution, Technical Report about the Progress of the Investigations on Gas Solid Pipe Flows, Project No. 7220-Ed/105, 1991, Erlangen

Authors address:
G. Živković
Laboratory for Thermal Engineering and Energy
VINČA Institute of Nuclear Sciences
P. O. Box 522, 11001 Belgrade, Yugoslavia

Paper submited: February 9, 1998
Paper revised: June 29, 1998
Paper accepted: February 2, 1999